Computer Prediction of Friction in Balloon Angioplasty and Stent Implantation

Denis Laroche[1], Sebastien Delorme[1], Todd Anderson[2], and Robert DiRaddo[1]

[1] Industrial Materials Institute, National Research Council Canada
75 de Mortagne, Boucherville, Quebec, Canada, J4B 6Y4
{denis.laroche, sebastien.delorme,
robert.diraddo}@cnrc-nrc.gc.ca
[2] University of Calgary, Dept. of Medicine
3330 Hospital Drive N.W., Alberta, Canada, T2N 4N1
todd.anderson@calgaryhealthregion.ca

Abstract. The success of balloon angioplasty and stent implantation depends on a balance between two conflicting objectives: maximization of artery lumen patency and minimization of mechanical damage. A finite element model for the patient-specific prediction of balloon angioplasty and stent implantation is proposed as a potential tool to assist clinicians. This paper describes the general methodology and the algorithm that computes device/artery interaction during stent deployment. The potential of the model is demonstrated with examples that include artery model reconstruction, device deployment, and prediction of friction on the arterial wall.

1 Introduction

Balloon angioplasty, the most practiced medical intervention worldwide, consists of dilating a stenosed artery with a polymeric balloon in order to restore blood flow to an acceptable level. Often, a stent is deployed and permanently implanted inside the artery to prevent elastic recoil of the artery. The most frequent complication of angioplasty, restenosis, is an excessive repair reaction of the arterial wall, related to its mechanical damage during the intervention. Restenosis has been shown to be related to two types of mechanical damage: 1) overstretch injury of the arterial wall and 2) denudation of the endothelium (the cell monolayer that lines the interior part of the arterial wall) due to friction with the balloon. The specific contribution of both types of injury to restenosis is still debated [1],[2]. Whether because of patients comeback after 6 months for target vessel revascularization or because of the use of expensive drug-eluting stents, it is generally recognized that restenosis increases by 25 to 30% the total cost of this intervention.

The success of angioplasty depends on a balance between two conflicting objectives: 1) maximizing the final deformation of the artery and 2) minimizing the mechanical damage to the arterial wall. Few research groups have attempted to simulate angioplasty with numerical or analytical models and predict its outcome. Angioplasty simulation, combined with current artery imaging technique such as intravascular

M. Harders and G. Székely (Eds.): ISBMS 2006, LNCS 4072, pp. 1 – 8, 2006.

ultrasound (IVUS), has the potential to become a clinical tool to assist in the selection of an appropriate intervention strategy for a specific patient. This could be done by virtually testing various strategies.

This work presents improvements to a finite element model for predicting the device/artery behavior during angioplasty [3],[4],[5]. These improvements consist of using pre-wrapped balloon models for saving computational time, and deploying both a balloon and stent inside an artery. Calculation of friction work is also proposed as a hypothesized predictor of endothelium denudation. To our knowledge, friction damage to the endothelium has never been considered in angioplasty simulations, possibly because of the difficulty of implementing a robust contact/slip algorithm for deforming bodies. An example of balloon angioplasty and stent implantation simulation on a coronary artery obtained from intravascular ultrasound imaging is presented to demonstrate the potential of the proposed model.

2 Methodology

A finite element modeling software developed for the analysis of large deformations of soft materials is used to solve angioplasty mechanics [3],[4],[5]. The model computes the device/artery interaction and large deformations that occur during device deployment into the diseased artery. It predicts the resulting artery lumen patency, including stress and strain distribution in the arterial wall, for a specific device and inflation pressure. It also predicts the amount of work done by the friction force on the arterial wall.

2.1 Multi-body Contact and Friction

Contact algorithms are usually time consuming and limiting factors in complex finite element applications. They have been traditionally used in explicit software and include collision detection [6],[7], non-penetration constraint and friction/slip capabilities [8],[9]. In this work a multi-body contact algorithm for implicit finite element computation is used [3]. Collisions between virtual nodes and surfaces moving with large displacement steps are detected with an implicit iterative approach that fully respects the non-penetration constraint. Once contact is detected, it is handled with an augmented Lagrange algorithm that computes slip and friction forces. The technique is stable for large displacement increments and is therefore directly applicable to finite deformation analysis.

It is assumed that the mechanical damage to the endothelium is related to the amount of friction exerted by the device during the intervention. In an effort to predict damage, the friction work per surface area is calculated. This value has the advantage of cumulating the amount of friction that occurs during the intervention. Equation 1 gives the friction work density Ω_f as a function of the history of the shear stress τ_f and relative velocity v between the two contacting surfaces.

$$\Omega_f = \int_{t=0}^{T} \vec{\tau}_f(t) \cdot \vec{v}(t) dt \quad (1)$$

The friction shear stress is a vector defined in Equation 2 where p is the contact pressure, μ is the friction coefficient, and v is the relative velocity between the two surfaces.

$$\vec{\tau}_f = p\mu \frac{\vec{v}}{\|\vec{v}\|} \tag{2}$$

2.2 Balloon Model

The angioplasty device model consists of a balloon wrapped around its longitudinal axis (Figure 1a). The balloon is modeled with triangular membrane elements and its mechanical properties are given by the Ogden hyperelastic constitutive equation [4]. The geometry of the wrapped balloon is constructed by mapping the nodes of the deployed balloon onto a wrapped configuration, as illustrated in Figure 1b. Points P_i on the deployed balloon of radius c are mapped onto points $\hat{P}_i$ of the folded balloon of inner radius a and outer radius b. Points P_i can be expressed in polar coordinates as (c,θ), and points $\hat{P}_i$ as $(\hat{r},\hat{\theta})$. A flap starts at point $\hat{P}_1$ and finishes at point $\hat{P}_2$. The angle β between P_1 and P_2 is calculated by Equation 3 where $\phi = 2\pi/n$.

$$\beta = \frac{\phi}{2}\left(\frac{b+a+2c}{b+a}\right) \tag{3}$$

The angle between $\hat{P}_1$ and $\hat{P}_2$ is given by:

$$\alpha = \frac{b+a}{2c}\beta \tag{4}$$

The angles and radii of points P_i are mapped onto points $\hat{P}_i$ using the following rule. If $\theta \in [0,\alpha]$ then

$$\hat{\theta} = \frac{\beta}{\phi}\theta \tag{5}$$

$$\hat{r}(\hat{\theta}) = a + \frac{b-a}{\beta}\hat{\theta} \tag{6}$$

If $\theta \in]\alpha,\beta]$ then

$$\hat{\theta} = \left(\frac{\beta-\phi}{\phi-\alpha}\right)(\phi-\theta)+\phi \tag{7}$$

$$\hat{r}(\hat{\theta}) = a + \frac{b-a}{\beta-\phi}(\hat{\theta}-\phi) \tag{8}$$

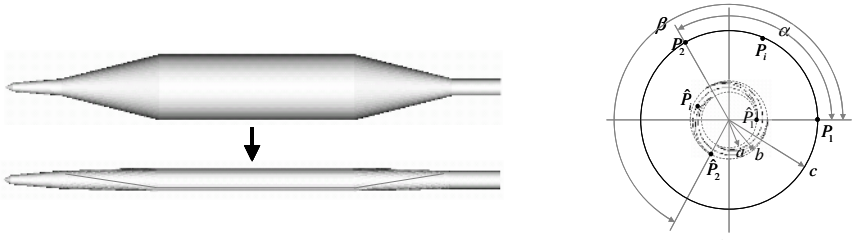

a) b)

Fig. 1. Balloon folding: a) balloon before and after folding; b) cross-section of balloon showing mapping of points from deployed configuration to wrapped configuration;

In this example an 8-mm long angioplasty balloon having a diameter of 2.7 mm was used. It was folded into a 3-ply configuration having an inner diameter of 0.7 mm and outer diameter if 1.0 mm. Balloon inflation occurs in two phases: 1) deployment and 2) stretching. Figure 2 illustrates three stages during the balloon deployment phase.

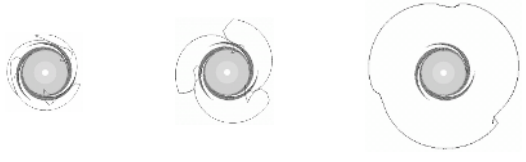

Fig. 2. Steps of balloon cross-section deployment

2.3 Stent Model

A three-dimensional model of a stent (Figure 3) was created using high resolution images of a crimped NIR Royal stent. The stent was meshed with 8-node hexahedral elements. The stainless steel behavior is modeled with a hyperelastic Mooney-Rivlin constitutive model. In order to overcome the high stress resulting from the use of an elastic model to simulate plastic deformation of stainless steel, a Young's Modulus of 6 GPa is used. The 6.2 mm long by 1.4 mm diameter stent is mounted over the balloon shown in Figure 1. Figure 3 shows the predicted deployment mechanics of the device. It can be seen that the extremities of the balloon inflate first. Even at 5 atm, the balloon is not completely deployed and a fold is still visible.

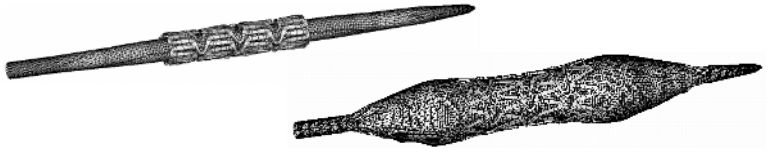

Fig. 3. Stent deployment

2.4 Artery Model

The artery model was reconstructed from intravascular ultrasound (IVUS) pullback images of a 39-mm long artery segment obtained during a percutaneous coronary

intervention (PCI). The 3D model of the artery was built using the Amira software (Mercury Computer Systems, Chelmsford, MA), from which an 11553-node mesh including tetrahedral elements was created [3]. Figure 4 shows a typical segmented image with identified lumen and media-adventitia borders.

The artery is modeled with incompressible solid elements and the Mooney-Rivlin hyperelastic constitutive model. The material constants (c_{10}=0.02, c_{01}=0.0) correspond to a homogeneous shear modulus of 0.04 MPa, as suggested in [10]. The use of an hyperelastic model instead of a more appropriate elasto-plastic has the major limitation of not allowing the prediction of the artery shape after the balloon is removed. However the mechanics of device deployment and its interaction with the arterial wall can be estimated. Tetrahedral elements rather than hexahedral elements are proposed for the artery, thus allowing the use of automatic mesh generation from medical images, and reducing the time required for pre-processing the data.

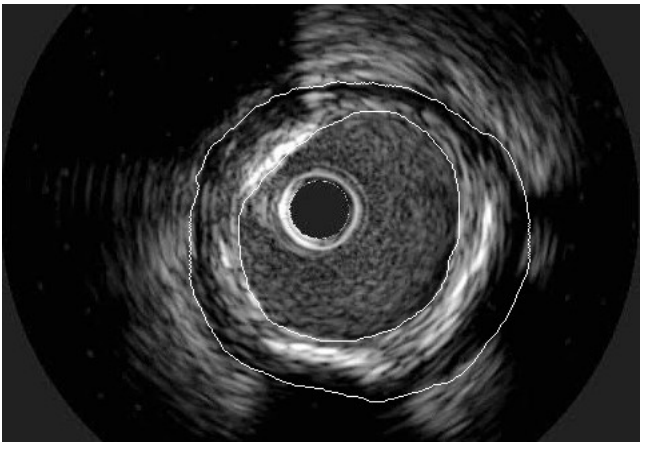

Fig. 4. Example of segmented IVUS image showing lumen and media-adventitia borders

3 Simulation Examples

Numerical simulations of balloon angioplasty and stent implantation in the mid-LAD coronary artery of a patient were performed at the most stenosed segment. In both cases, the extremities of the artery and the device were fixed and the device was slightly stretched axially.

3.1 Balloon Angioplasty

Figure 5 shows predicted balloon inflation steps at 1.4 atm and 5 atm of inflation pressure. It can be observed that contact between the balloon and arterial wall occurs during the deployment phase of the balloon inflation, involving friction slip. Because of boundary conditions applied on the balloon and artery, the balloon deployment is considerably affected by the artery shape and that the slip between the balloon and the artery is important.

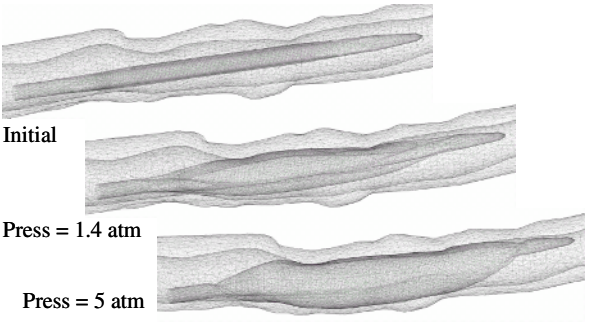

Fig. 5. Balloon angioplasty inside an artery, from 0 to 5 atm inflation pressure

3.2 Direct Stenting

The stent model shown in Figure 3 was deployed inside the same artery segment. Figure 6 shows the deployment at an inflation pressure of 2.8 atm and 10 atm. It can be seen that a much higher pressure is required to re-open the artery due to the presence of the stent.

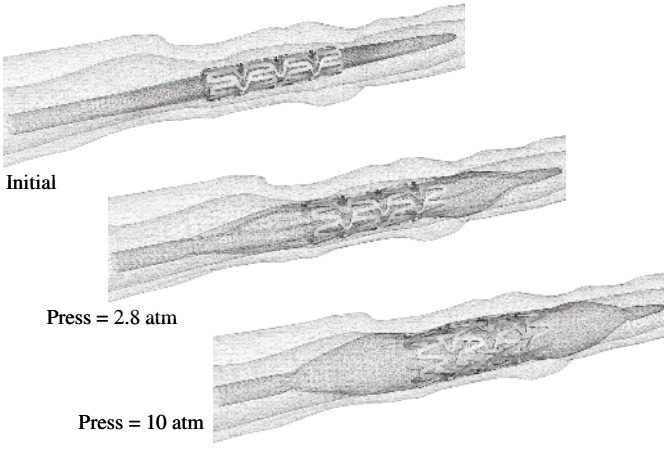

Fig. 6. Deployment of stent inside an artery

As it was the case with unconfined balloon/stent deployment (Figure 3), the extremities of the balloon are inflated first. This implies that the extremities of the stent might be the first to contact the artery. Compared with the predicted balloon angioplasty of the previous example, the balloon deploys into a more regular shape when a stent is present.

3.3 Prediction of Friction Work

The friction work density Ω_f was integrated over the artery inner surface to obtain the cumulative work of the friction force on the endothelium. Figure 7 shows its

evolution as a function of the inflation pressure for both the balloon angioplasty and the stent implantation.

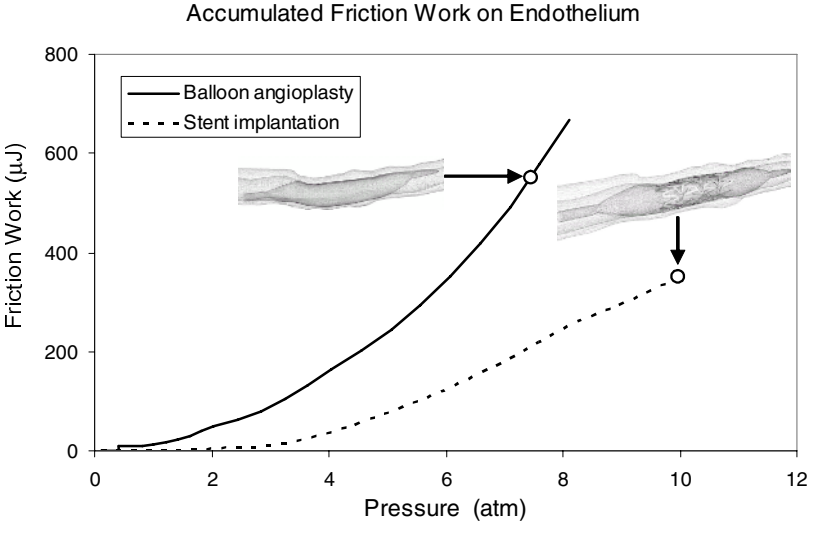

Fig. 7. Predicted cumulative friction work on the arterial wall for balloon angioplasty and stent implantation

Friction is expected to occur during the two phases of balloon inflation. First, during balloon deployment, the balloon flaps slip against the arterial wall. Second, when the balloon is fully deployed, it might start to stretch uniformly while the artery would stretch non-uniformly because of uneven thickness, explaining why friction work continues to increase after the balloon is fully deployed.

The predicted friction work on the endothelium is lower in the presence of the stent, possibly because the friction occurred mostly between the balloon and the stent. This could potentially indicate that stent deployment results in less endothelium damage than balloon angioplasty.

4 Conclusion

In this paper a finite element model for predicting balloon angioplasty and stent implantation from artery imaging was presented. It demonstrated that balloon angioplasty and stent implantation mechanics differ. Most notably, the presence of the stent constrained the balloon to a slower and more symmetrical deployment than when the balloon is deployed alone.

The proper modeling of the interaction between the balloon, the stent and the artery allowed predicting friction work on the endothelium. The presence of the stent resulted in a reduced friction work, suggesting that the stent might protect the artery against friction damage.

Future work will focus on constitutive models for the artery and the use of deformable catheters to further improve the accuracy of the simulation. Experimental work is underway to quantify the relationship between friction work and endothelial denudation. Also, predicted artery response after device removal will also be validated using post-intervention imaging data.

References

1. Clowes, A.W., Clowes, M.M., Fingerle, J., Reidy, M.A.: Kinetics of cellular proliferation after arterial injury. V. Role of acute distension in the induction of smooth muscle proliferation, Lab Invest, Vol. 60 (1989) 360-364
2. Fingerle, J., Au, Y.P., Clowes, A.W., Reidy, M.A.: Intimal lesion formation in rat carotid arteries after endothelial denudation in absence of medial injury, Arteriosclerosis, Vol. 10 (1990) 1082-1087
3. Laroche, D., Delorme, S., Anderson, T., Buithieu, J., DiRaddo, R.: Computer Prediction of Balloon Angioplasty from Artery Imaging, Medicine Meets Virtual Reality 14, J.D. Westwood et al. (Eds), Technology and Informatics, Vol .119 (2006) 293-298
4. Delorme, S., Laroche, D., DiRaddo, R., Buithieu, J.: Modeling polymer balloons for angioplasty: from fabrication to deployment, Proc Annual Technical Conference, ANTEC, SPE, Chicago, IL (2004)
5. Laroche, D., Delorme, S., Buithieu, J., DiRaddo, R.,: A three-dimentional finite element model of balloon angioplasty and stent implantation, Proc Comp Meth Biomech Biomed Eng, Vol. 5, Madrid (2004)
6. Hallquist, J.O., Goudreau, G.L., Benson, D.J.: Sliding interfaces with contact-impact in large-scale lagrangian computations, Comp Meth App Mech Eng, Vol. 51 (1985) 107-137
7. Zhong, Z.H.: Finite element procedures for contact-impact problems. Oxford University Press (1993)
8. Laursen, T.A., Simo, J.C.: A continuum-based finite element formulation for the implicit solution of multibody, large deformation frictional contact problems. Int J Num Meth Eng, Vol. 36 (1993) 3451-3485
9. Puso, M.A., Laursen, T.A.: A mortar segment-to-segment contact method for large deformation solid mechanics. Comp Meth Appl Mech Eng, Vol. 193 (2004) 601-629
10. Holzapfel, G.A., Stadler, M., Schulze-Bauer, C.A.J.: A layer-specific three-dimensional model for the simulation of balloon angioplasty using magnetic resonance imaging and mechanical testing, Ann. Biomed. Eng., Vol. 30 (2002) 753-767